The American Journal of Human Genetics, Volume *105*

Supplemental Data

Mutations in *TTC29*, Encoding an Evolutionarily Conserved Axonemal Protein, Result in Asthenozoospermia and Male Infertility

Patrick Lorès, Denis Dacheux, Zine-Eddine Kherraf, Jean-Fabrice Nsota Mbango, Charles Coutton, Laurence Stouvenel, Come Ialy-Radio, Amir Amiri-Yekta, Marjorie Whitfield, Alain Schmitt, Caroline Cazin, Maëlle Givelet, Lucile Ferreux, Selima Fourati Ben Mustapha, Lazhar Halouani, Ouafi Marrakchi, Abbas Daneshipour, Elma El Khouri, Marcio Do Cruzeiro, Maryline Favier, François Guillonneau, Marhaba Chaudhry, Zeinab Sakheli, Jean-Philippe Wolf, Catherine Patrat, Gérard Gacon, Sergey N. Savinov, Seyedeh Hanieh Hosseini, Derrick R. Robinson, Raoudha Zouari, Ahmed Ziyyat, Christophe Arnoult, Emmanuel Dulioust, Mélanie Bonhivers, Pierre F. Ray, and Aminata Touré

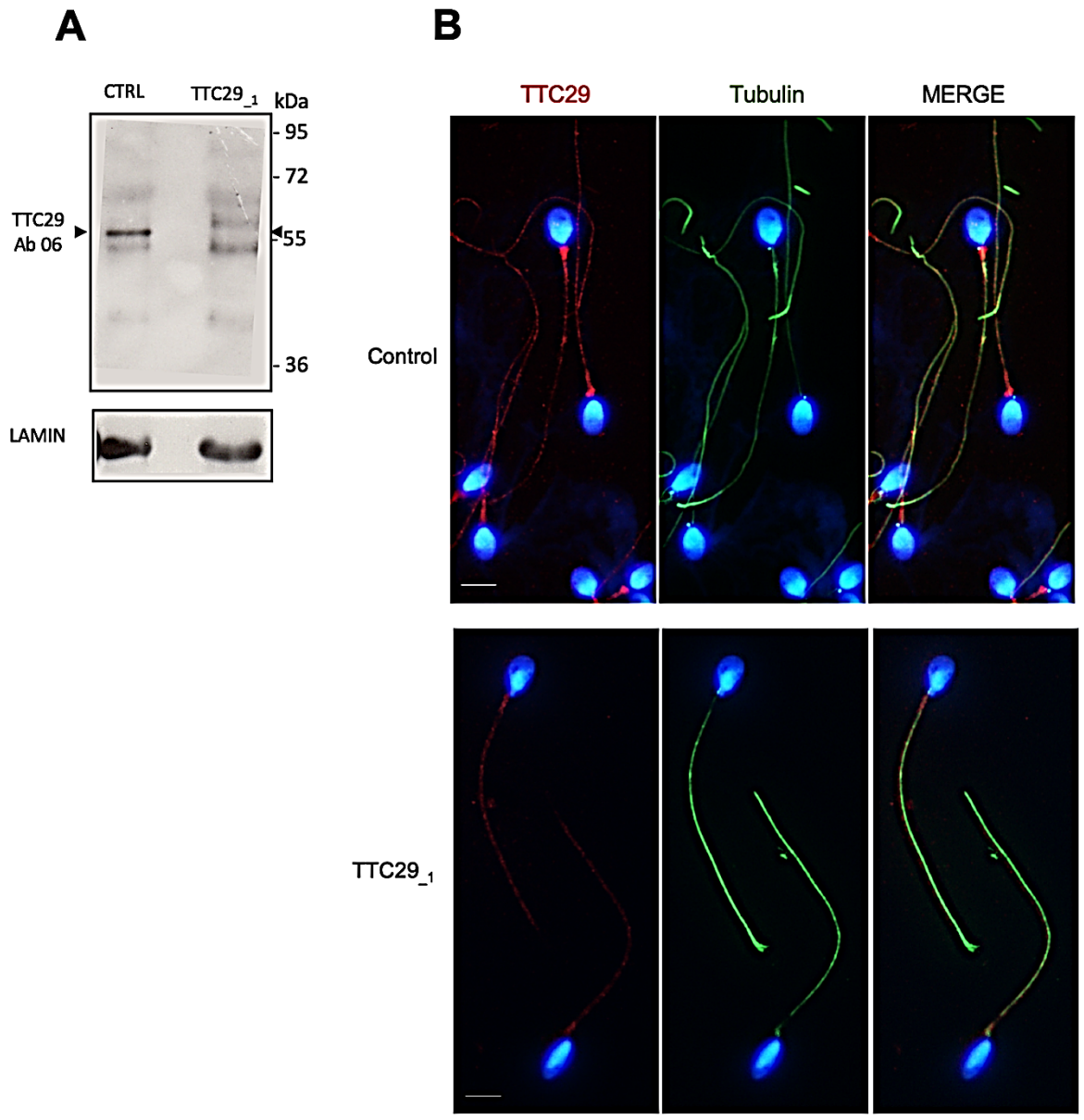

Figure S1. Functional consequences of the c.176 +1G>A *TTC29* variant on TTC29 protein amount and distribution.
(A) Western blot on semen samples from control and individual TTC29_1, carrying the c.176 +1G>A mutation, using a the TTC29 (06) antibody (SIGMA HPA037006). Lamin antibody was used for loading control. **(B)** Immunodetection on semen samples from control and individual TTC29_1, carrying the c.176 +1G>A mutation, using a the TTC29 (Ab73) antibody. TTC29 antibody (in red) and Tubulin (in green). Cells were counterstained with DAPI (in blue) as nuclei marker. Scale bars represent 5µm.

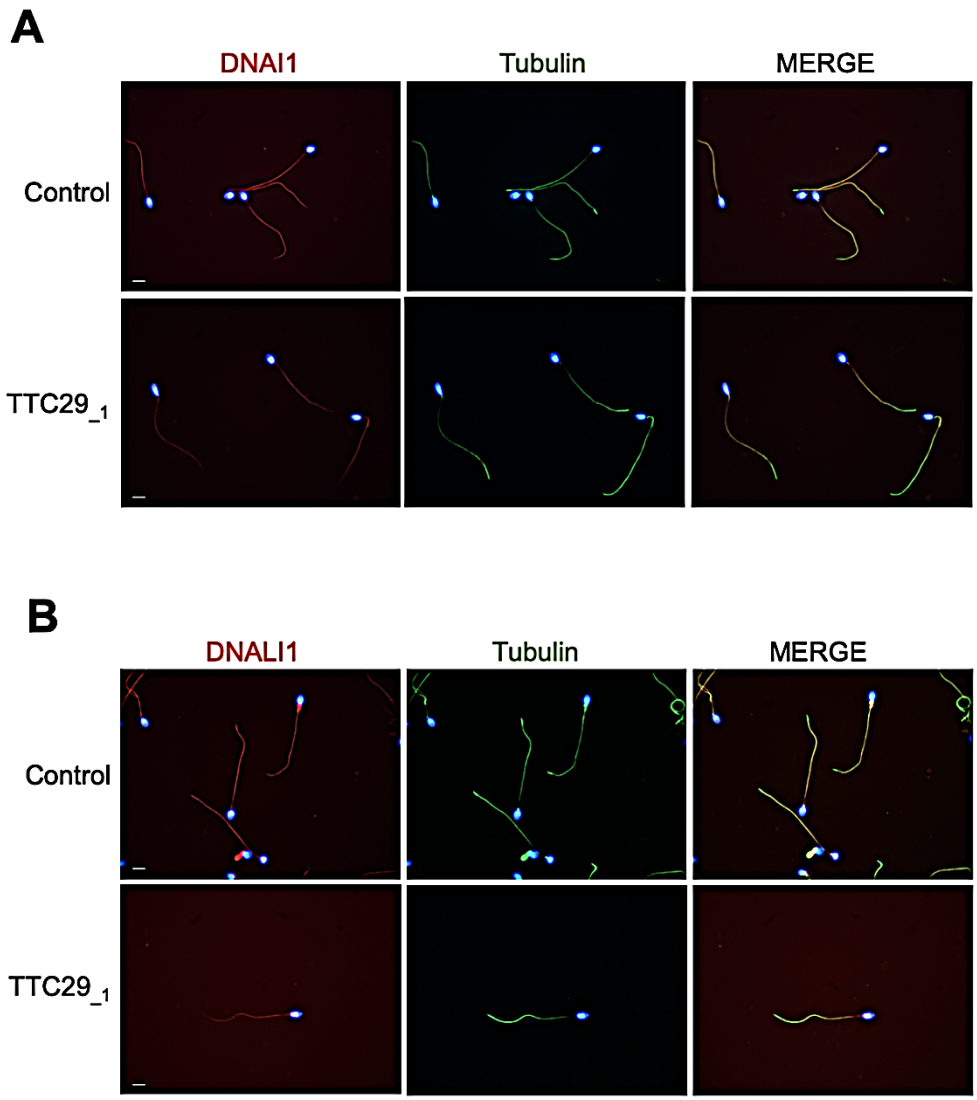

Figure S2. Immunostaining of DNAI1 and DNALI1 in spermatozoa from control individual and individual TTC29_1, carrying the c.176 +1G>A mutation.

(**A**) Immunofluorescence staining of spermatozoa from control and from individual TTC29_1 with DNAI1 (an intermediate chain of Outer dynein Arms, ODAs, in red) and α-Tubulin (in green). (**B**) Immunofluorescence staining of spermatozoa from control and from individual TTC29_1 with DNALI1 (an associated protein of Inner dynein Arms, IDAs, in red) and α-Tubulin (in green). Spermatozoa were counterstained with DAPI (blue) as nuclei marker. Scale bars represent 5µm.

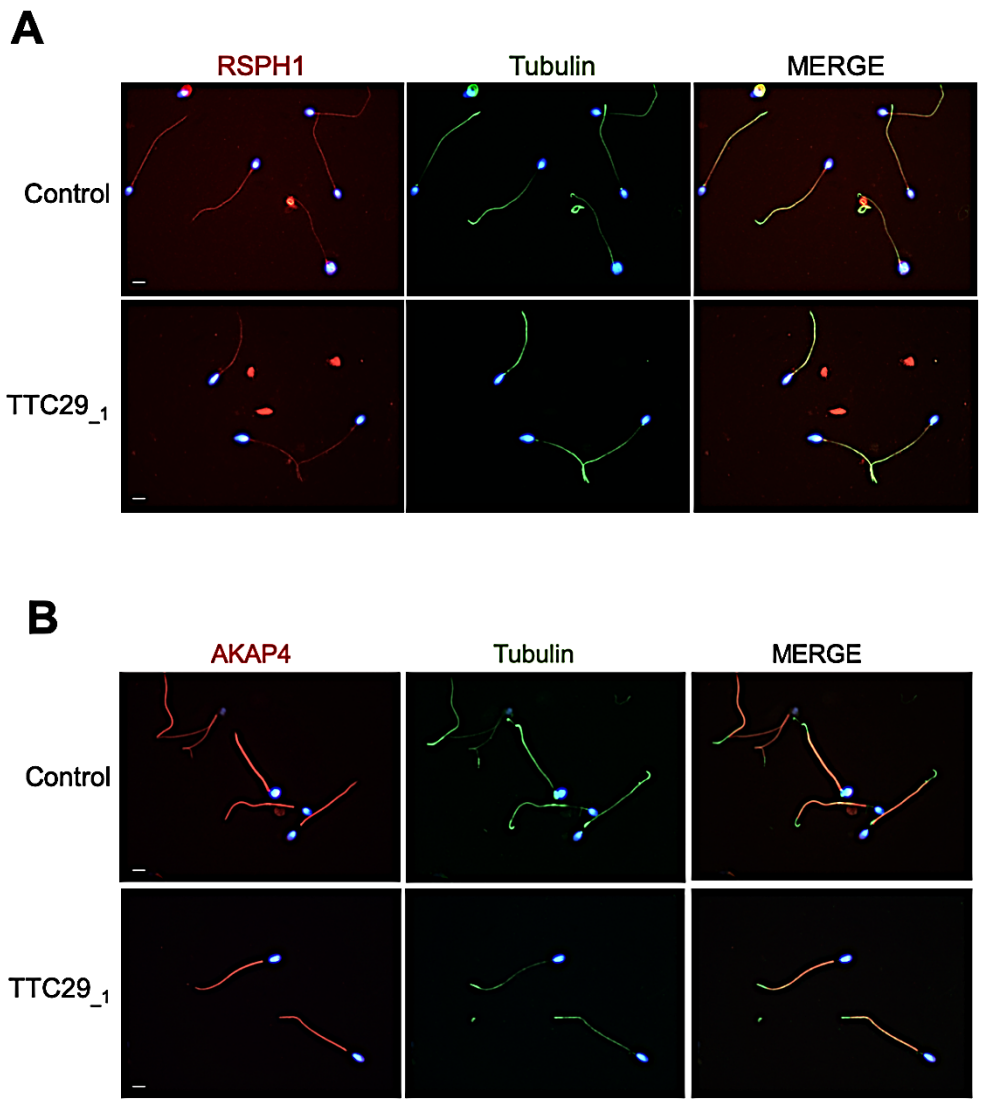

Figure S3. Immunostaining of RSPH1 and AKAP4 in spermatozoa from control individual and individual TTC29$_{_1}$, carrying the c.176 +1G>A mutation.

(**A**) Immunofluorescence staining of spermatozoa from control and from individual TTC29$_{_1}$ with RSPH1 (a component of Radial Spokes, RSs, in red) and α-Tubulin (in green). (**B**) Immunofluorescence staining of spermatozoa from control and from individual TTC29$_{_1}$ with AKAP4 (a component of the Fibrous Sheath, FS, in red) and α-Tubulin (in green). Spermatozoa were counterstained with DAPI (blue) as nuclei marker. Scale bars represent 5µm.

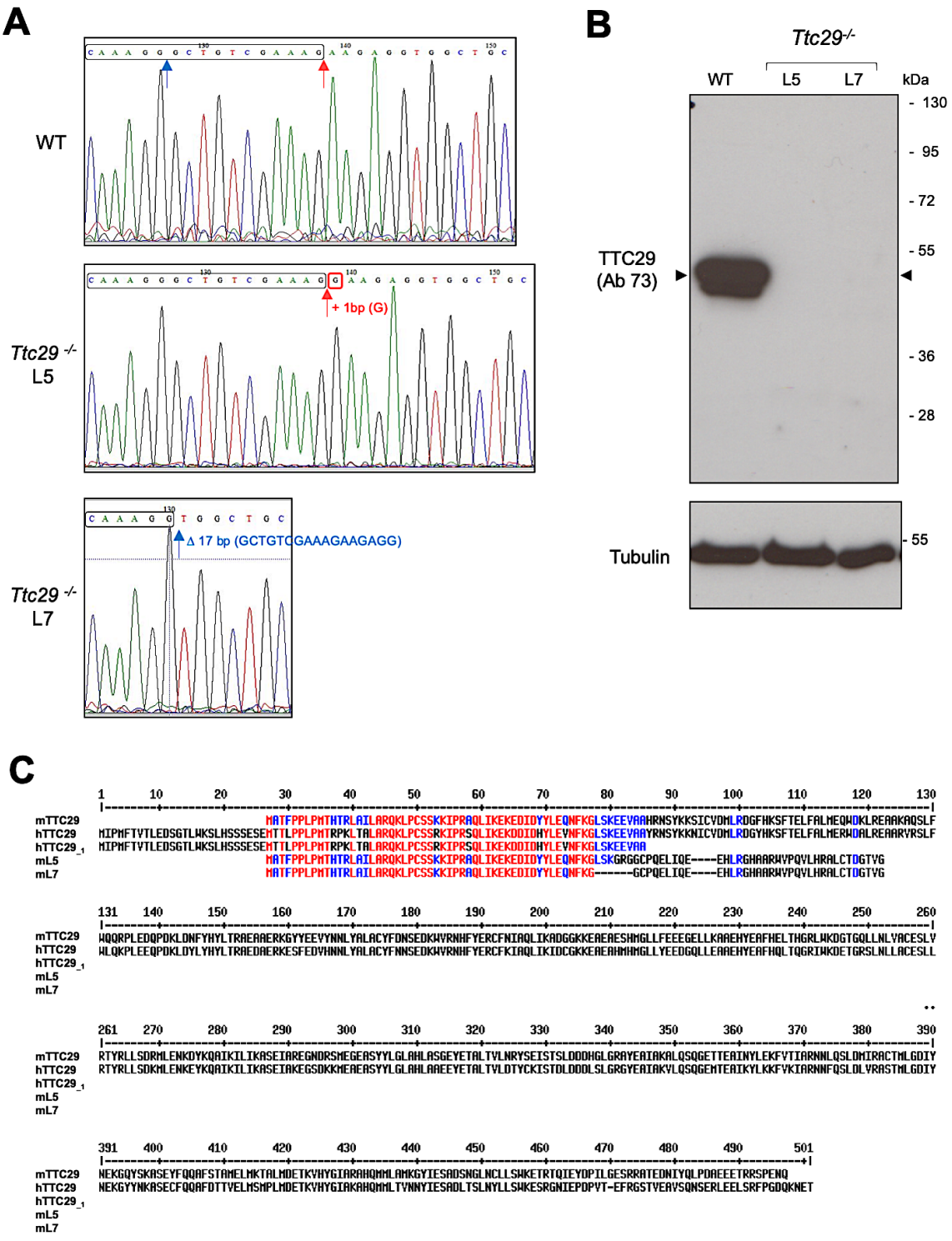

Figure S4. Generation of *Ttc29* mutant mice by CRISPR-Cas9 gene editing technology.
(A) Sanger sequencing of genomic DNA from *Ttc29*$^{-/-}$ L5 and L7 mutant mice compared to control mouse. The chromatograms show the insertion of one base in *Ttc29* exon 5 for the *Ttc29*$^{-/-}$ L5 mutant line and the deletion of 17 bases in *Ttc29* exon 5 for the *Ttc29*$^{-/-}$ L7 mutant line. **(B)** Western blot analysis of testis protein extracts from *Ttc29*$^{-/-}$ L5 and L7 mutant mice using TTC29 (73) antibody directed against the N-terminus of the protein, which show the absence of protein. Tubulin was used as loading control. **(C)** Sequence alignment of the predicted encoded proteins in *Ttc29*$^{-/-}$ L5 and L7 mutant mice (mL5 and mL7, respectively) compared to wild-type mouse and human TTC29 proteins (mTTC29 and hTTC29, respectively) and the theoretical truncated protein resulting from the c.176 +1G>A splicing mutation in individual TTC29$_{_1}$ (hTTC29$_{_1}$).

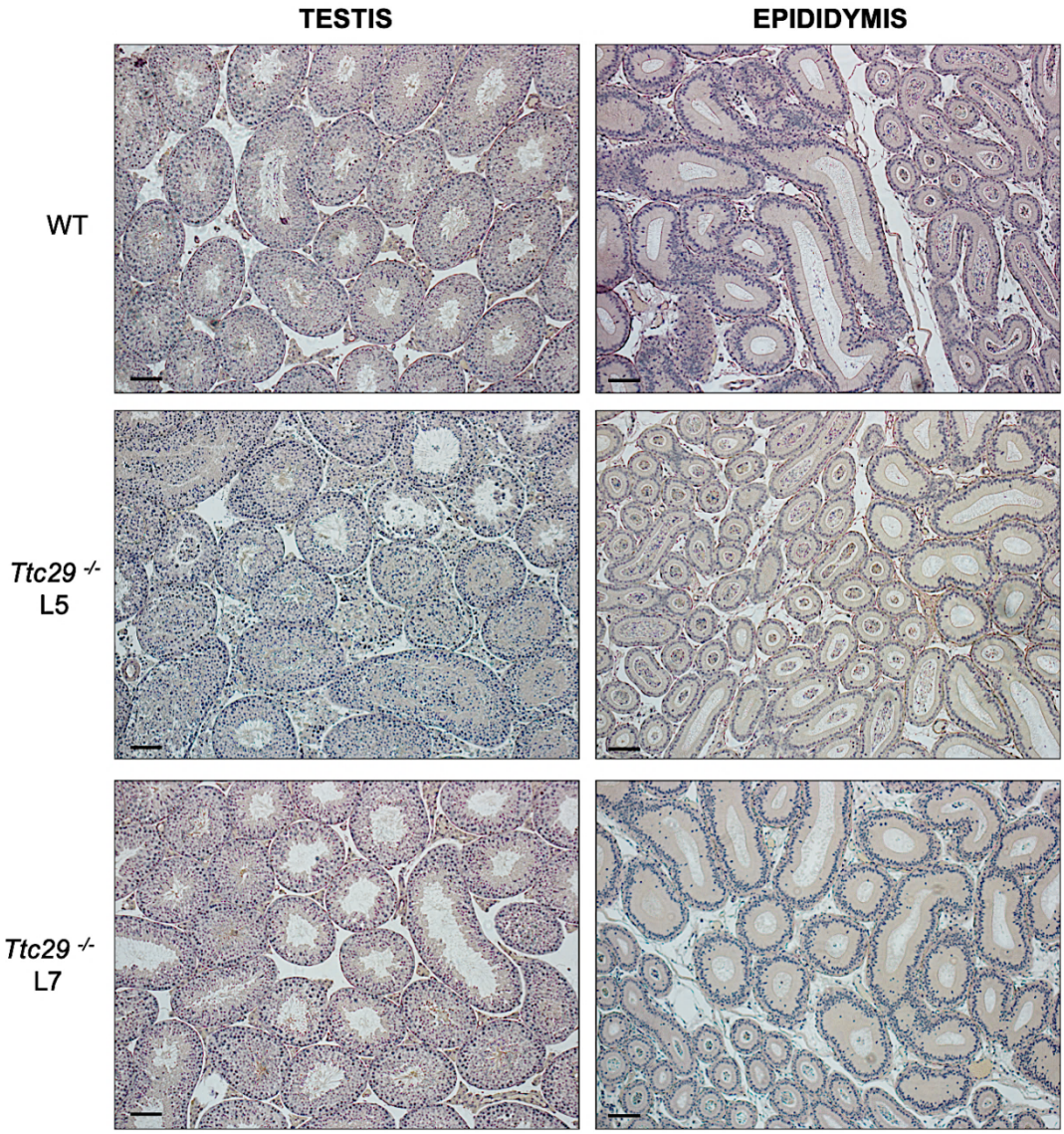

Figure S5. Histological analysis of testes and epididymides from *Ttc29*$^{-/-}$ L5 and L7 mutant mice. Hematoxylin and eosin staining of testes and epididymides from *Ttc29*$^{-/-}$ L5 and L7 mutant mice. Scale bars indicate 50μm.

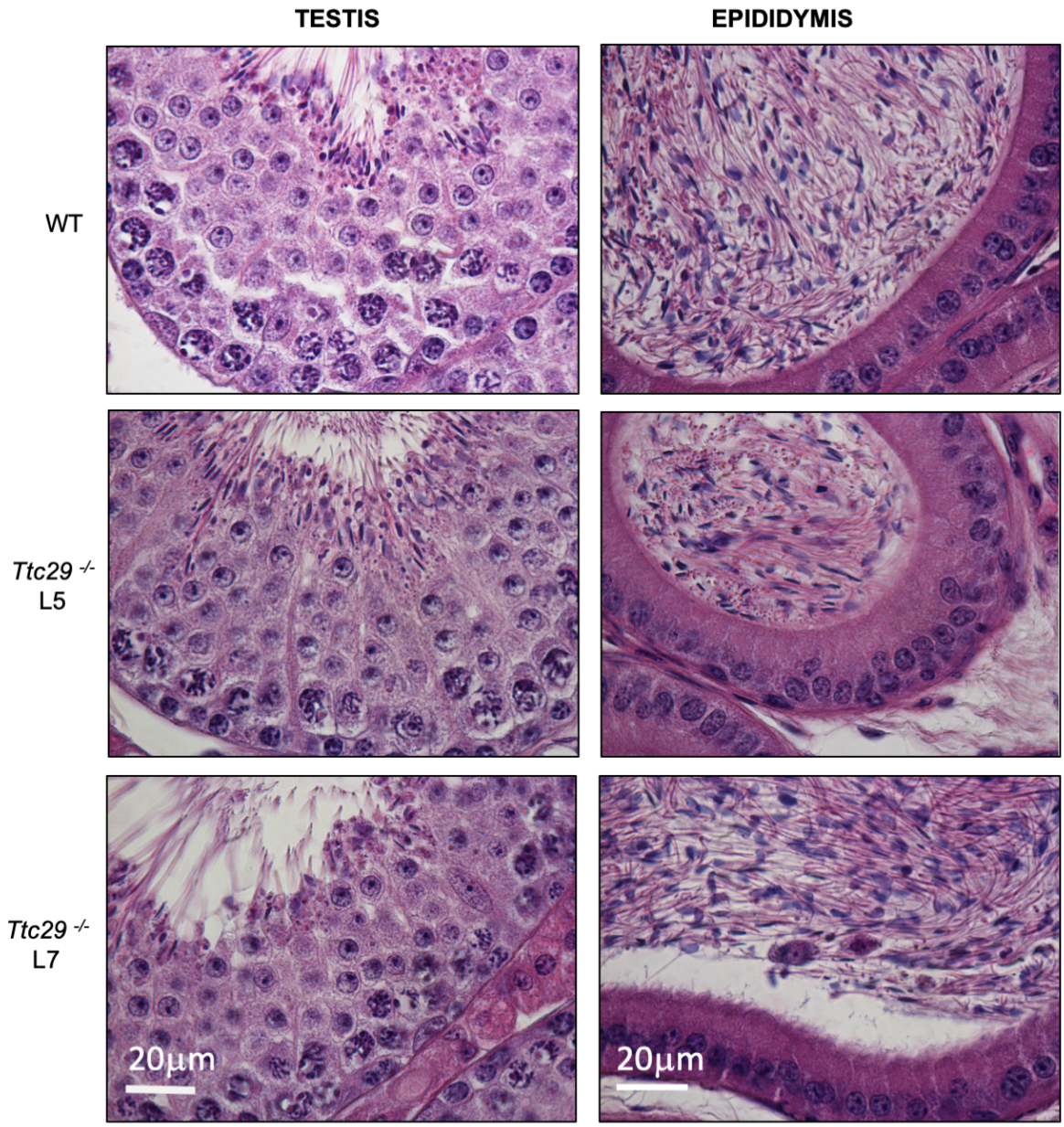

Figure S6. High magnification of testis tubule and epididymis section from *Ttc29*$^{-/-}$ L5 and L7 mutant mice. Hematoxylin and eosin staining of testes and epididymides from *Ttc29*$^{-/-}$ L5 and L7 mutant mice. Scale bars indicate 20µm.

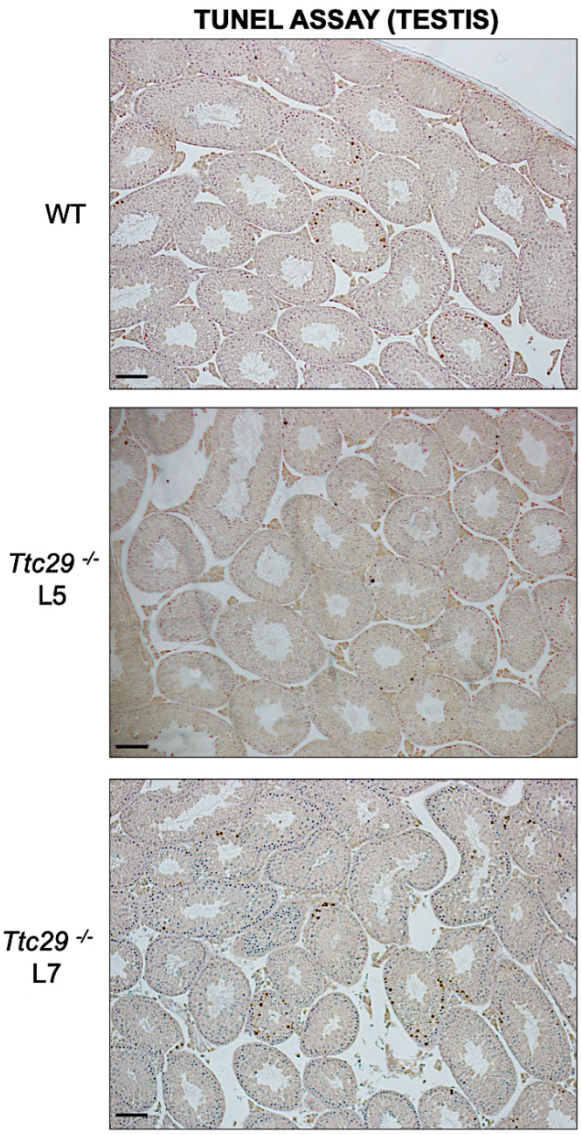

Figure S7. Detection of apoptotic cells in testes from *Ttc29*$^{-/-}$ L5 and L7 mutant mice.
Testes paraffin embedded sections processed for TUNEL assay. Scale bars indicate 50µm.

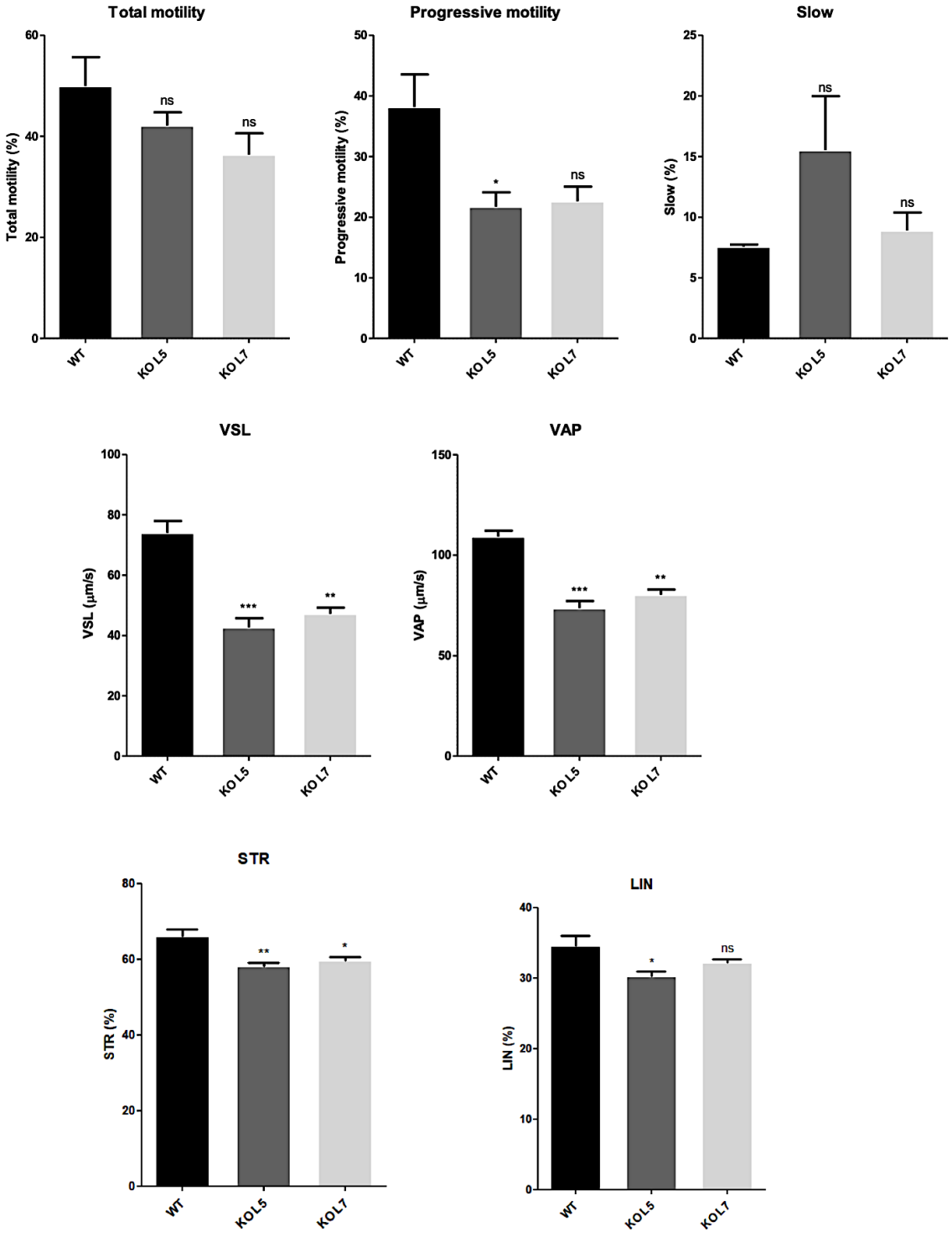

Figure S8. Assessment of sperm motility parameters of *Ttc29*$^{-/-}$ L5 and L7 mutant mice using Computer Aided Sperm Analysis (CASA).

Sperm kinematic movements of *Ttc29*$^{-/-}$ L5 and L7 mutant mice were measured using CASA system (CEROS II, Hamilton). N=3 for each genotype. The following parameters are reported: percentage of motile cells (total motility), percentage of progressive cells (progressive motility), percentage of slow cells, straight-line velocity (VSL), average-path velocity (VAP), straightness (STR) and linearity (LIN). Data are represented as the mean ± SEM. p-value <0.05 (*); p-value <0.01 (**); p-value <0.001 (***); non-significative (ns).

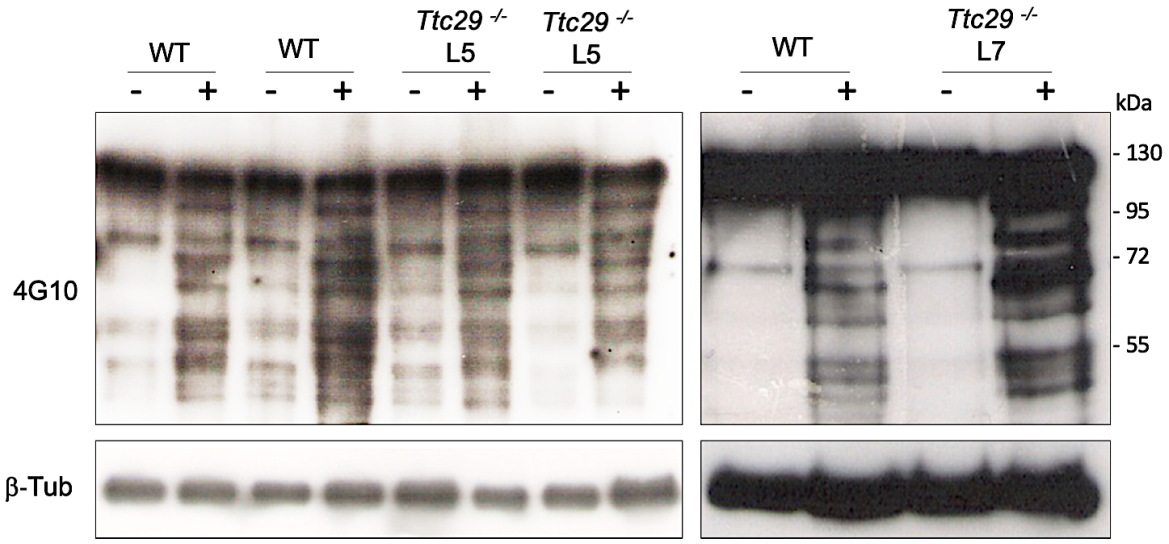

Figure S9. Evaluation of the capacitation-associated tyrosine-phosphorylation profile of *Ttc29*$^{-/-}$ L5 and L7 mutant sperm.

Spermatozoa from control (WT) and *Ttc29*$^{-/-}$ L5 and L7 mutant mice were retrieved from cauda epididymes and incubated in non-capacitating medium (-) or medium supporting capacitation (+). Anti-phosphotyrosine immunoblotting was performed with 4G10 antibody. Tubulin (β-Tub) was used as loading control.

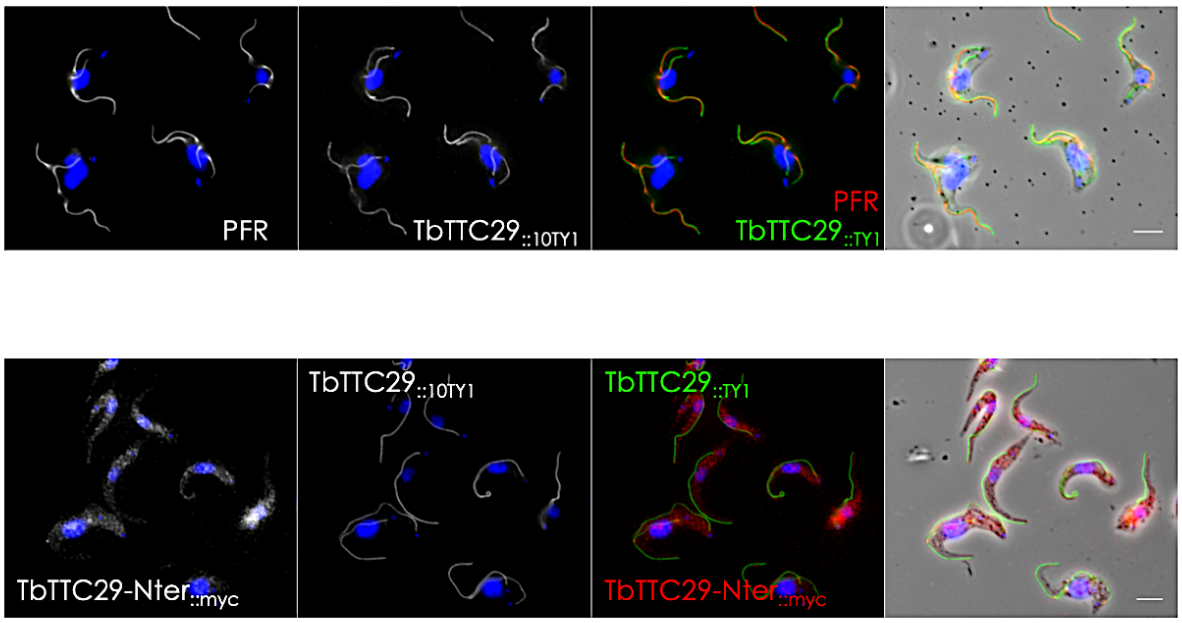

Figure S10. Localization of TbTTC29 in T. brucei cell lines.
Low magnification pictures of TbTTC29::TY1 (upper panel) and TbTTC29::TY1/TbTTC29-Nter::myc (lower panel) immunolabelling with anti-PFR (red), anti-Myc (red) and anti-TY1 (green) antibodies. The mitochondrial genome and the nuclei are stained with DAPI. Scale bars represent 5 μm.

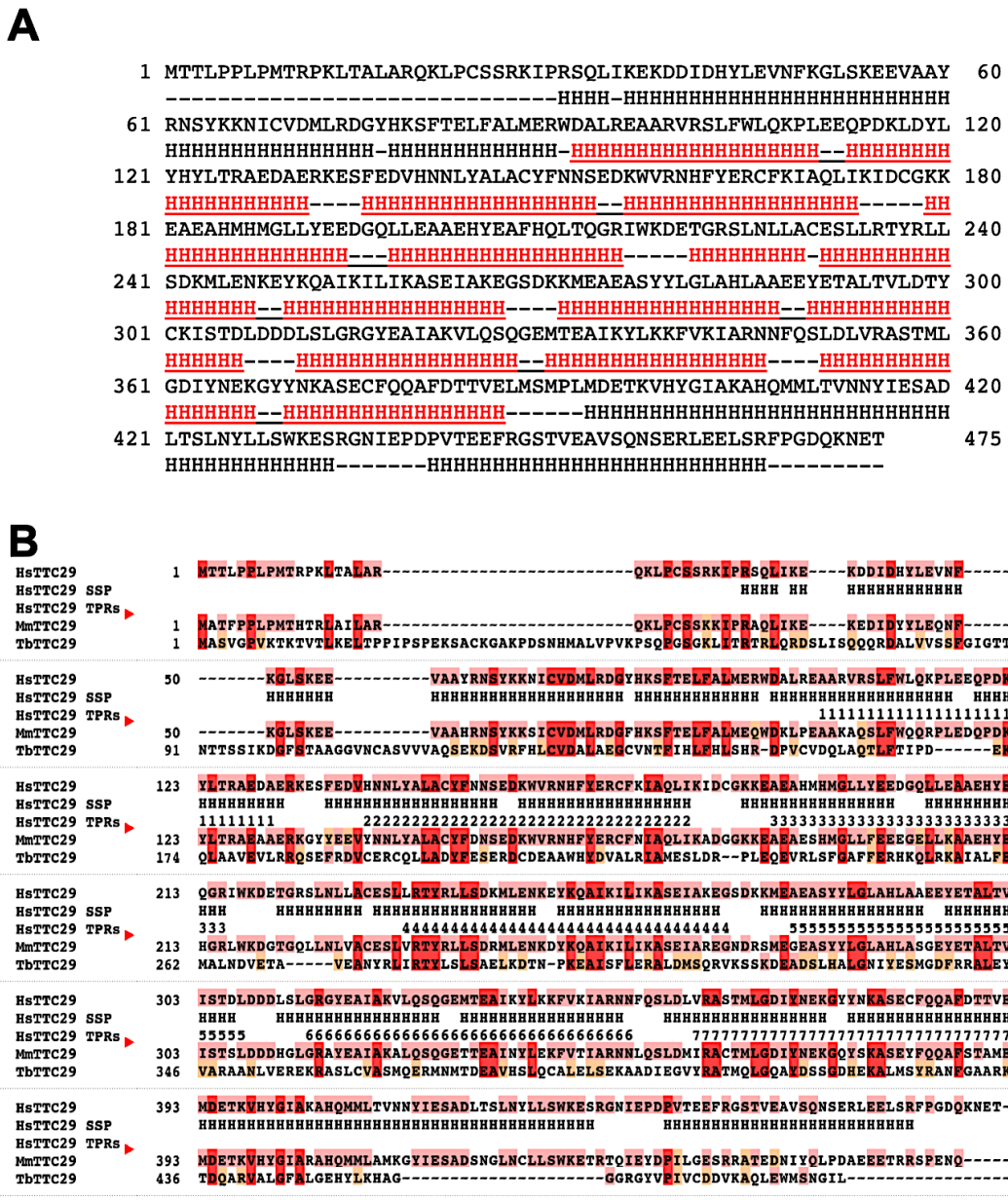

Figure S11. TPR domains identification and structural homology between HsTTC29, MmusTTC29 and TbTTC29 proteins

(A). Identification of 7 pairs of helices of 36-40 amino-acids each, compactly disposed throughout the central part of human TTC29 protein, and flanked by unpaired N-terminal and C-terminal helices, by means of secondary structure prediction (JPred4) and manual alignment of suspect peptides. Pair and unpaired α-helical residues (H) are marked in red and black, respectively. (**B).** TTC29 protein alignment from human (HsTTC29), mouse (MmusTTC29) and T. Brucei (TbTTC29) showing α-helical residues (H) identified by secondary structure prediction (SSP, JPred4). Numbers designate TPR repeats 1 to 7 identified in HsTTC29; fully conserved, partially conserved and similar residues are red, pink and orange, respectively. Sequence alignment was performed using the blastp suite of BLAST (Basic Local Alignment Search Tool) for non-redundant protein sequences (https://blast.ncbi.nlm.nih.gov/Blast.cgi). The sequences were processed and rendered using Multiple Sequence Viewer tool within Maestro.

Primer name	Primer sequence (5'-3')	Tm	Product size (bp)
TTC29_Ex5-F1	CTCCTGGTGGCATTTTATGTGT	60°C	378
TTC29_Ex5-R1	GGTAAATATGGGAATTTTGAGAGCCA		
TTC29_Ex6-F1	TGTGGACATGCTGCGAGATG	60°C	426
TTC29_Ex6-R1	TGTGTTGTCTTCCCTGGCTC		

Table S1. Primer sequences used for Sanger sequencing verification of *TTC29* mutations and respective melting temperatures (Tm) and product sizes.

Primer name	Primer sequences (5'-3')	Tm	Product size (bp)
hTTC29_RT-fw3	GAAGCTTACAGCCTTAGCC	60°C	264
hTTC29_RT-rv4	ACTCTCGCAGCCTCCCTC		

Table S2. Primers used for RT-PCR of TTC29 in human samples and respective melting temperatures (Tm) and product sizes.

Antibody	Species	End-use	WB dilution	IF dilution	Provider & Reference
Human and Mouse studies					
TTC29 (Ab 06)	Rabbit	Primary	1/100		Sigma HPA037006
TTC29 (Ab 73)	Rabbit	Primary	1/400	1/100	Sigma HPA061473
4G10	Mouse	Primary	1/1000		Sigma-Upstate 05-321
AKAP4	Rabbit	Primary		1/400	Sigma HPA020046
DNAI1	Rabbit	Primary		1/100	Sigma HPA021649
DNALI1	Rabbit	Primary		1/100	Sigma HPA028305
SPAG6	Rabbit	Primary		1/200	Sigma HPA038440
α-Tubulin	Mouse	Primary		1/500	Sigma T9026
β-Tubulin	Mouse	Primary	1/5000		Sigma-Upstate 05-661
Lamin B1	Mouse	Primary	1/500		Life 33-2000
Rabbit-Ig HRP	Swine	Secondary	1/1000		DAKO P0217
Mouse-Ig HRP	Rabbit	Secondary	1/1000		DAKO P0260
Rabbit-Ig Alexa 568	Goat	Secondary		1/500	Thermofischer A11036
Mouse-Ig Alexa 488	Goat	Secondary		1/250	Thermofischer A11001
Trypanosome studies					
Anti-TY1 tag (BB2)	Mouse	Primary	1/5000	1/200	P. Bastin
Anti-myc tag	Rabbit	Primary	1/1000	1/1000	Sigma C-3956
Anti-mouse HRP		Secondary	1/10000		Jackson 515-035-062
Anti-rabbit HRP		Secondary	1/10000		Sigma A-9169
Anti-PFR2 (L8C4)	Mouse	Primary	1/1000		K. Gull
Anti-enolase	Rabbit	Primary	1/10000		F. Bringaud
Anti-FTZC	Rabbit	Primary		1/10000	F. Bringaud
Anti-PFR2	Rabbit	Primary		1/2000	N. Biteau
Anti-mouse FITC	Goat	Secondary		1/100	Sigma F-2012
anti-rabbit Alexa594	Goat	Secondary		1/100	Thermofischer A11012

Table S3. Antibodies used for western blot (WB) and immunofluorescence (IF).

Primer name	Primer sequences (5'-3')	Tm	Product size (bp)
TTC29_scr-fw	CTGATGTGTCTTCTCTTCTGG	60°C	443
TTC29_ scr-rv	TAATAGCTCAGACTTAACTCAAT		

Table S4. Primers used for screening of *Ttc29* CRIPR mutant mice and respective melting temperatures (Tm) and product sizes

	Primer name	Primer sequences (5'-3')
TbTTC29 endotagging	1321-F-TbTTC29	CGGGGGGAGGACGCGGATATGTGCCAATTGTATGTGATGATGTAAAGGCACAACTAGAGTGGATGAGTAATGGCATCTTG ggttctggtagtggttcc
	1322-R-TbTTC29	CGTCTCCCCCCCCCAAAAAAAAAAAACCTCCTCACCCTTCCGAGAATAAACAGATAAATCCTCCTTCGGATCGTCACCAA ccaatttgagagacctgtgc
TbTTC29-Nter endotagging	1321-F-TbTTC29	CGGGGGGAGGACGCGGATATGTGCCAATTGTATGTGATGATGTAAAGGCACAACTAGAGTGGATGAGTAATGGCATCTTG ggttctggtagtggttcc
	1339-F-TbTTC29-DCter	CCTCTATCAAAGATGGATTTTCCACCGCTGCCGGGGGCGTTAACTGCGCGTCGGTTGTGGTGGCACAAAGTGAAAAGGAC ggttctggtagtggttcc
RNAi	841-F-TTC29rnai	GCCGGCCGCTCTAGAgatggattttccaccgctgcc
	842-R-TTC29rnai	TAAGCTTGCTCTAGAgcaccaaacgacaaacgcacc

Table S5. Primers used for TbTTC29, TbTTC29-Nter endotagging and for the RNAi construct.

	228 WT	228p WT	470 WT	471 WT	227 KO L5	227p KO L5	479 KO L5	488 KO L7
ACTMLGDIYNEK	822440 [1]	1138000 [3]	217930 [2]	267560 [1]	0	0	0	0
AHQMMLAMK	0	192340 [2]	336170 [2]	408230 [2]	0	0	0	0
ALQSQGETTEAINYLEK	3351400 [3]	3564400 [3]	1397800 [2]	989570 [2]	0	0	0	0
ASEYFQQAFSTAMELMK	0	0	0	123260 [1]	0	0	0	0
AYEAIAK	3126200 [2]	3788300 [2]	3971400 [3]	648640 [1]	**41600 [1]**	0	0	0
CFNIAQLIK	**271230 [1]**	169320 [1]	693210 [2]	990080 [1]	0	0	0	0
DGTGQLLNLVACESLVR	680510 [4]	1438100 [4]	2056100 [4]	2040200 [4]	0	0	0	0
EKEDIDYYLEQNFK	2102400 [1]	0	0	**812300 [2]**	0	0	0	0
GYIESADSNGLNCLLSWK	221440 [1]	0	0	458180 [1]	0	0	0	0
NNLQSLDMIR	3840000 [3]	4006500 [2]	2839900 [1]	2578100 [1]	0	0	0	0
TALMDETK	3196700 [1]	3369700 [1]	2862600 [1]	**2165400 [1]**	0	0	0	**619110 [1]**
TQIEYDPILGESR	2605400 [2]	2865700 [2]	3347200 [2]	4053100 [2]	0	0	0	0
YSEISTSLDDDHGLGR	4574100 [2]	4046600 [3]	2619500 [3]	4213000 [4]	0	0	0	0

Table S6. TTC29 peptides identification by tandem mass spectrometry (MS/MS) analysis on purified flagella preparations from control and *TTC29*$^{-/-}$ L5 and L7 mutant sperm.

Tandem mass spectrometry (MS/MS) analysis was performed on purified flagella preparations from control (WT) and *TTC29*$^{-/-}$ L5 and L7 KO sperm. N=4 for controls and N=4 for *TTC29*$^{-/-}$ mutants. For each TTC29 peptide identified, the Label-Free Quantification intensity (LFQ) is reported and the number of times the peptide was identified is indicated in brackets. Peptides which were not directly identified by MS/MS but uncovered by Match Between Runs (MBR) are indicated in bold characters.

The position of all identified peptides is indicated below, in bold characters, in the TTC29 mouse protein sequence; the position of the mutation in the crispr mutant mouse lines is indicated by the arrow.

MATFPPLPMTHTRLAILARQKLPCSSKKIPRAQLIK**EKEDIDYYLEQNFK**▼GLSKEEVAAHRNSYKKSI
CVDMLRDGFHKSFTELFALMEQWDKLPEAAKAQSLFWQQRPLEDQPDKLDNFYHYLTRAEAAERK
GYYEEVYNNLYALACYFDNSEDKWVRNHFYER**CFNIAQLIK**ADGGKKEAEAESHMGLLFEEEGELL
KAAEHYEAFHELTHGRLWK**DGTGQLLNLVACESLVR**TYRLLSDRMLENKDYKQAIKILIKASEIAR
EGNDRSMEGEASYYLGLAHLASGEYETALTVLNR**YSEISTSLDDDHGLGRAYEAIAKALQSQGETT
EAINYLEK**FVTIAR**NNLQSLMIRACTMLGDIYNEK**GQYS**KASEYFQQAFSTAMELMKTALMDET
KVHYGIARAHQMMLAMKGYIESADSNGLNCLLSWK**ETR**TQIEYDPILGESR**RATEDNIYQLPDA
EEETRRSPENQ

PROTEIN	228 WT	228p WT	470 WT	471 WT	227 KO	227p KO	479 KO	488 KO	p-value
DNAI1	181370000	168860000	106510000	102320000	143230000	169540000	96107000	139330000	0,973976 (ns)
DNALI1	193290000	201340000	236420000	212420000	166060000	209250000	167240000	212400000	0,204586 (ns)
RSPH1	52203000	57131000	56484000	74144000	55574000	57388000	65614000	89196000	0,476173 (ns)
SPAG6	143730000	135270000	172810000	144230000	147200000	150620000	127570000	159020000	0,801091 (ns)
TTC29	21310000	21801000	22040000	24310000	0	0	0	0	0,000117 (**)

Table S7. Axonemal protein identification by tandem mass spectrometry (MS/MS) analysis on purified flagella preparations from control and *TTC29*$^{-/-}$ L5 and L7 mutant sperm.
Tandem mass spectrometry (MS/MS) analysis was performed on purified flagella fractions from wild type (WT) and *TTC29*$^{-/-}$ L5 and L7 KO sperm. N=4 for controls and N=4 for *TTC29*$^{-/-}$ mutants. The Label-Free Quantification intensity (LFQ) for identified peptides matching the protein sequence of DNAI1, DNALI1, RSPH1 and SPAG6 and TTC29, is reported for each animal. t-student test was performed to compare the LFQ of the tested protein between WT and KO genotypes. In contrast to TTC29, which was not detected in flagella preparations from the mutant mice, all axonemal proteins were present in similar amount than in the wild type preparations. p-value <0.01 (**); non-significative (ns).

Supplemental material and methods

Western blot analysis on human sperm cells or mouse testis extracts

Denaturized protein samples corresponding to equal amounts of human spermatozoa or mouse testis extracts were loaded on SDS-PAGE (12% acrylamide/bisacrylamide (40% 37.5:1)) and transferred onto nitrocellulose membranes as previously described [1; 2]. The membranes were blocked in 5% milk in PBS-Tween 0.1% or 3% BSA in TBS-Tween 0.1%, and immunoblot analysis was performed using the indicated primary antibodies. Details of antibodies and dilutions used for western blot assays are provided in Table S4.

Immunofluorescence analysis of human sperm cells

10 µl of semen samples were spread onto a Superfrost Plus slide (Menzel Glasbearbeitungswerk, GmbH & Co. KG, Braunschweig, Germany). Sperm was fixed by incubation with PBS/4% paraformaldehyde for 10 minutes. The slides were incubated 20 minutes at 95°C in citrate buffer (H-3300, VectorLabs, Burlingame, CA, USA). The slides were next treated with 0.2% Triton in PBS for permeabilization and then blocked by incubation in 1% BSA for 1 hour. They were then incubated with primary antibodies for 2 hours at room temperature and then secondary antibodies for one hour at room temperature. The slides were mounted in Vectashield medium (Vector Laboratories, Burlingame, USA) supplemented with 0.5 µg/ml DAPI. Slides were analyzed with a Zeiss Axiophot epifluorescence microscope. Digital images were acquired with a cooled charge-coupled device (CCD) camera (Hamamatsu Co. Japan), under identical instrument settings, with MetaMorph® software (Molecular Devices, Inc. USA). Details of antibodies and dilutions used for immunofluorescence assays are provided in Table S4.

Histological analysis of mouse testes and epididymes

Testes and epididymides from wild type and mutant mice were dissected out and immediately fixed in Davidson's modified buffer for 1 up to 4 hours at room temperature. Fixed tissues were then dehydrated, embedded in paraffin, sectioned at 5 µm. Sections were rehydrated and stained with hematoxylin and eosin. Digital images were acquired with EVOS™ XL Cell Imaging System. Images were further analyzed using ImageJ software.

TUNEL analysis on mouse sperm

Testes paraffin embedded sections were processed for TUNEL assay using the TACS 2 Tdt DAB kit (Trevingen, Gaithersburg, USA), following manufacturer's instructions. DNA fragmentation in apoptotic cells was detected in situ after peroxidase staining by the TdT-mediated dUTP-biotin end-labeling procedure. For statistical analysis, TUNEL-positive cells were counted in at least 200 seminiferous tubules for each animal.

Mouse sperm motility analysis

Sperm motility was assessed by Computer Aided sperm Analysis (CASA) using CEROS II apparatus (Hamilton Thorne, Beverly, MA USA). Briefly, mouse sperm cells expelled from the cauda epididymis were recovered into M2 medium (Sigma-Aldrich, Saint-Louis, MO, USA). The movements of at least 500 sperm cells per sample were analyzed in 20 µm chambers (Leja Products B.V., Netherlands) with Zeiss AX10 Lab. A1 microscope (10x objective), using HT CASAII software. The settings were as follows: acquisition rate, 60 Hz; number of frames, 45; minimum head brightness, 175; minimum tail brightness, 80; minimum head size, 10 µm2; minimum elongation gate, 1%; maximum elongation gate, 100%; objective magnification factor, 1.2. The percentage of motile cells (total motility), percentage of

progressive cells (progressive motility), percentage of slow cells, straight-line velocity (VSL), average-path velocity (VAP), straightness (STR) and linearity (LIN) were recorded. Progressive sperm cells were characterized by average path velocity (VAP)>45µm/s and straightness (STR=VSL/VAP)>45%, respectively.

Mouse sperm capacitation analysis

Spermatozoa from control (WT) and *Ttc29*$^{-/-}$ L5 and L7 mutant mice were retrieved from cauda epididymides in medium not supporting capacitation (-). Sperm were then diluted to 2 million spermatozoa in 400 µl of the appropriate medium: medium not supporting capacitation (-) or medium containing 1.8mM calcium, 25 mM bicarbonate and 3% albumin, supporting capacitation (+), and incubated during 90 min at 37°C, under an atmosphere containing 5% CO2 (as previously described[3]). Spermatozoa were washed 3 times with PBS containing a phosphatase inhibitor cocktail (PhosStop, Roche) and protein were extracted and denaturated in Laemmli buffer (4% SDS, 20% glycerol, 10% β-mercaptoethanol, 0.004% bromophenol blue, 0.125 MTris–HCl). For Western blot analysis, proteins were resolved by sodium dodecyl sulfate–polyacrylamide gel electrophoresis (SDS–PAGE) (2 × 106 cells/lane) and transferred to nitrocellulose membranes for anti-phosphotyrosine immunoblotting with 4G10 antibody. Tubulin (β-Tub) was used as loading control.

Mouse sperm flagella purification

Spermatozoa were retrieved from mouse epididymides cauda and flagella were purified following previously described protocoles [4]. Briefly, the caudal regions of mouse epididymis were dissected in 1 mL of NO medium (NaCl 120mM, KCl 2mM, MgSO4 1,2mM, NaH2PO4 0.36mM, Glucose 5,56mM, Sucrose 18,5mM, Hepes 50mM, NaPyruvate 1mM, pH 7,3) and incubated at 37°C for 15 min. The sperm cells suspension was distributed in 3 tubes (0.3 ml/tube) and sonicated using Diagenode® Bioruptor Pico (3 x 20 seconds of sonication with 1 minute of cooling between each sonication run). Each sample of 0.3 ml was then loaded on 1 ml of 80 % Percoll and centrifuged at 650g during 35 minutes at 4 °C. The top 0,3 mL was discarded and the following 0.2 ml corresponding to the enriched sperm tail fraction was collected, diluted in 1 mL of cold PBS and centrifuged at 16,000g for 70 minutes at 4 °C. The sperm tail enriched pellets were washed once more time with 1 mL of cold PBS and then frozen at -80°C. Quality and purity of the preparations were assessed by microscopic examination.

Proteomics analysis using label free quantification

Purified sperm tail pellets were lysed in 25 µl 100 mM TRIS/HCl pH8.5 containing 10 mM TCEP, 40 mM chloroacetamide and 1% sodium deoxycholate, sonicated 3 times and incubated for 5 minutes at 95°C. 20µg of protein lysate were diluted (1:1) in TRIS 25mM pH 8.5 in 10% Acetonitrile (ACN) and subjected to trypsin digestion with 0.4 µg of sequencing-grade bovine trypsin (Promega) overnight at 37°C. Peptides were separated from deoxycholate using liquid-liquid phase extraction with 50µL of 1% TriFluoroacetic Acid (TFA) in ethyl-acetate using a six layer home-made Stagetip with Empore disks Styrene- divinylbenzene - Reversed Phase. Sulfonate (SDB RPS) (from 3M). Eluted and dried peptides were solubilized in 2% TFA and fractionated in 5 fractions by hand-made Strong Cation eXchange (SCX) StageTips [5] and analyzed using an U3000 RSLC nanochromatographer eluting into an Orbitrap Fusion mass spectrometer (both from Thermo Scientific). Briefly: peptides from each SCX fraction were separated on a C18 reverse phase column (2µm particle size, 100 Å pore size, 75µm inner diameter, 25cm length) with a 145 minutes gradient starting from 99% of solvent A containing 0.1% formic acid in H_2O, ending in 40% of solvent B containing 80% ACN and 0.085% formic acid in H_2O. The MS1 scans spanned from 350-1500 m/z with 1.10^6 Automated Gain Control (AGC) target, within 60ms

maximum ion injection time (MIIT) and a resolution setting of 60,000. In a 3 seconds window, as many Higher energy Collisional Dissociation (HCD) dynamic exclusion time of 30s. Precursor selection window was set at 1.6 m/z with quadrupole filtering. HCD Normalized Collision Energy was set at 30% and the ion trap scan rate was set to "rapid" mode with AGC target 1.10^5 and 60ms MIIT. The mass spectrometry data were analyzed using Maxquant (v.1.6.1.0) [6]. The database used was a concatenation of human sequences from the Uniprot-Swissprot database (release 2017-05) and the list of contaminant sequences from Maxquant. Cystein carbamidomethylation was set as constant modification and acetylation of protein N-terminus and oxidation of methionine were set as variable modifications. Second peptide search and the "match between runs" (MBR) options were allowed. Label-free protein quantification (LFQ) was done using both unique and razor peptides with at least 2 such peptides required for LFQ. Raw quantitative data quality was evaluated using PTXQC software v. 0.92.3 [7]. Statistical analysis and data comparison were done using the Perseus software version 1.6.2.3 [8].

Supplemental references

1. Lores, P., Coutton, C., El Khouri, E., Stouvenel, L., Givelet, M., Thomas, L., Rode, B., Schmitt, A., Louis, B., Sakheli, Z., et al. (2018). Homozygous missense mutation L673P in adenylate kinase 7 (AK7) leads to primary male infertility and multiple morphological anomalies of the flagella but not to primary ciliary dyskinesia. Hum Mol Genet 27, 1196-1211.
2. Lores, P., Vernet, N., Kurosaki, T., Van de Putte, T., Huylebroeck, D., Hikida, M., Gacon, G., and Toure, A. (2014). Deletion of MgcRacGAP in the male germ cells impairs spermatogenesis and causes male sterility in the mouse. Dev Biol 386, 419-427.
3. Rode, B., Dirami, T., Bakouh, N., Rizk-Rabin, M., Norez, C., Lhuillier, P., Lores, P., Jollivet, M., Melin, P., Zvetkova, I., et al. (2012). The testis anion transporter TAT1 (SLC26A8) physically and functionally interacts with the cystic fibrosis transmembrane conductance regulator channel: a potential role during sperm capacitation. Hum Mol Genet 21, 1287-1298.
4. Hashemitabar, M., Sabbagh, S., Orazizadeh, M., Ghadiri, A., and Bahmanzadeh, M. (2015). A proteomic analysis on human sperm tail: comparison between normozoospermia and asthenozoospermia. J Assist Reprod Genet 32, 853-863.
5. Kulak, N.A., Pichler, G., Paron, I., Nagaraj, N., and Mann, M. (2014). Minimal, encapsulated proteomic-sample processing applied to copy-number estimation in eukaryotic cells. Nat Methods 11, 319-324.
6. Cox, J., Hein, M.Y., Luber, C.A., Paron, I., Nagaraj, N., and Mann, M. (2014). Accurate proteome-wide label-free quantification by delayed normalization and maximal peptide ratio extraction, termed MaxLFQ. Mol Cell Proteomics 13, 2513-2526.
7. Bielow, C., Mastrobuoni, G., and Kempa, S. (2016). Proteomics Quality Control: Quality Control Software for MaxQuant Results. J Proteome Res 15, 777-787.
8. Tyanova, S., Temu, T., Sinitcyn, P., Carlson, A., Hein, M.Y., Geiger, T., Mann, M., and Cox, J. (2016). The Perseus computational platform for comprehensive analysis of (prote)omics data. Nat Methods 13, 731-740.